Since January 2020 Elsevier has created a COVID-19 resource centre with free information in English and Mandarin on the novel coronavirus COVID-19. The COVID-19 resource centre is hosted on Elsevier Connect, the company's public news and information website.

HOSTED BY

ELSEVIER

Available online at www.sciencedirect.com

ScienceDirect

Radiology of Infectious Diseases 7 (2020) 55−61

www.elsevier.com/locate/jrid

Research article

Quantitative computed tomography of the coronavirus disease 2019 (COVID-19) pneumonia

Zenghui Cheng [a,1], Le Qin [a,1], Qiqi Cao [a], Jianyi Dai [b,*], Ashan Pan [c], Wenjie Yang [a], Yaozong Gao [d], Lei Chen [d], Fuhua Yan [a]

[a] *Department of Radiology, Ruijin Hospital, Shanghai Jiao Tong University School of Medicine, Shanghai 200025, China*
[b] *Department of Infectious Diseases, Wenzhou Central Hospital, Wenzhou, Zhejiang 325000, China*
[c] *Department of Radiology, Yueqing People's Hospital, Yueqing, Zhejiang 325600, China*
[d] *Shanghai United Imaging Intelligence Healthcare Co., Ltd. Shanghai 150200, China*

Received 24 March 2020; revised 17 April 2020; accepted 23 April 2020
Available online 28 April 2020

Abstract

Objective: To quantify coronavirus diseases 2019 (COVID-19) pneumonia and to explore whether quantitative computer tomography (CT) could be used to assess severity on admission.
Materials and methods: From January 17 to February 9, 2020, 38 hospitalized patients with COVID-19 pneumonia were consecutively enrolled in our hospitals. All clinical data and the chest CT on admission were retrospectively reviewed and analyzed. Firstly, a quantitative method based on multi-scale convolutional neural networks was used to assess the infected lung segments and this was compared with the semi-quantitative method. Secondly, the quantitative method was tested with laboratory results and the pneumonia severity index (PSI) by correlation analyses. Thirdly, both quantitative and semi-quantitative parameters between patients with different PSI were compared.
Results: Thirty cases were finally enrolled: 16 (53.33%) of them were male, and the mean age was 48 years old. The interval from onset symptoms to first chest CT scan was 8 days. The proportion of ground glass opacity (GGO), consolidation and the total lesion based on the quantitative method was positively correlated with the semi-quantitative CT score ($P < 0.001$ for all; $rs = 0.88, 0.87, 0.90$), CRP ($P = 0.0278$, 0.0168, 0.0078; $rs = 0.40, 0.43, 0.48$) and ESR ($P = 0.0296$, 0.0408, 0.0048; $rs = 0.46, 0.44, 0.58$), respectively, and was negatively correlated with the lymphocyte count ($P = 0.0222$, 0.0024, 0.0068; $rs = -0.42, -0.53, -0.48$). There was a positive correlation trend between the proportion of total infection and the pneumonia severity index ($P = 0.0994$; $rs = 0.30$) and a tendency that patients with severe COVID-19 pneumonia had higher percentage of consolidation and total infection ($P = 0.0903$, 0.0989).
Conclusions: Quantitative CT may have potential in assessing the severity of COVID-19 pneumonia on admission.

Keywords: Computed tomography; Quantitative; Novel coronavirus; COVID-19; Viral pneumonia

1. Introduction

Pneumonia caused by the severe acute respiratory syndrome coronavirus 2 (SARS-CoV-2) has been reported since last December in Wuhan, Hubei province, China [1−3]. Patients infected with SARS-CoV-2 can develop a condition called coronavirus diseases 2019 (COVID-19), which can lead to severe pneumonia, acute respiratory distress syndrome, multiple organ failure and even death; therefore, detection of

* Corresponding author. Department of Infectious Diseases, Wenzhou Central Hospital, Wenzhou, Zhejiang 325000, China
E-mail address: daijianyi2008@163.com (Jianyi Dai).
Peer review under responsibility of Beijing You'an Hospital affiliated to Capital Medical University.
[1] These two authors made equal contributes.

https://doi.org/10.1016/j.jrid.2020.04.004

the infection is pivotal, as is making an early initial assessment so that subsequent planning of appropriate treatment and careful follow-up can be prepared in advance.

Preliminary studies on imaging features of patients with the COVID-19 found that bilateral, multifocal ground glass opacity (GGO) and consolidation, predominantly located at subpleural and peri-bronchovascular regions, were the typical features [4,5]. Suspicion of COVID-19 would be high in patients with fever, typical imaging features and contact history. Two case−control cohort studies found that for the factors associated with severity certain clinical characteristics and laboratory results differed between hospitalized patients in intensive care unit (ICU) and those not in ICU [6,2], suggesting that these characteristics might be used as predictors for the severity. Previous investigations into severe acute respiratory syndrome (SARS) and middle-east respiratory syndrome (MERS) reported the number of involved lung segments might be used as a predictor [7,8], which indicates that quantitative imaging might also be used as a method to assess severity. As quantitative computer tomography (CT) using a deep learning algorithm might have better performance and efficiency than the traditional semi-quantitative method based on visual score, in this study we intend to explore whether the quantitative method could have potential in assessing the severity of the COVID-19 pneumonia on admission.

2. Material and methods

2.1. Study participants

This retrospective study was approved by our Institutional Review Board and written informed consent was waived. 38 patients were consecutively collected from January 17th to February 9th, 2020 in our hospitals. The criteria included were as follows: ① symptoms of viral infection: fever, cough, sore throat, rhinorrhea, short of breath, chest pain, muscle ache, nausea and vomiting and diarrhea, ② normal or reduced total leukocytes or lymphocyte count, ③ imaging manifestations of pneumonia, ④ history of epidemiological, ⑤ positive result of real-time polymerase chain reaction (RT−PCR) test either from throat-swab, sputum or blood specimen. The excluded criteria were as follows: ① patients without thin-sectional chest CT, ② patients without pneumonia on chest CT but with positive result of RT−PCR, ③ chest CT with severe movement artifacts. Of these 38 patients, 2 with negative chest findings, 5 with 5-cm-thickness chest CT and 1 with severe movement artifact were excluded, and 30 patients with COVID-19 pneumonia were finally included for further analyses. Patients were also grouped into different subgroups based on the severity of COVID-19 pneumonia.

2.2. Clinical data analysis

All clinical data on demographics, signs and symptoms, and laboratory results were retrospectively reviewed (Table 1). The pneumonia severity index (PSI) score system [9] was used to assess the severity of the COVID-19 pneumonia on admission.

Table 1
Baseline characteristics of the 30 patients with COVID-19 pneumonia.

Characteristics	Normal range	Number (%)
Age (years)		48.00 ± 11.38
Gender	Male	16 (53.33)
	Female	14 (46.67)
Exposure		30 (100.00)
Onset symptoms to 1st CT, median (IQR)		8 (6.0−10.5)
Comorbidities	Hypertension	8 (26.67)
	Diabetes	3 (10.00)
Signs and symptoms	Tmax (ºC)	23 (76.67)
Fever		37.74 ± 0.99
Cough		20 (66.67)
Phlegm		12 (40.00)
Chills		6 (20.00)
Headache		6 (20.00)
Muscle ache		3 (10.00)
Chest tightness		3 (10.00)
Sore throat		2 (6.67)
Chest ache		2 (6.67)
Diarrhea		2 (6.67)
Shortness of breath		1 (3.33)
Nausea and vomiting		1 (3.33)
SpO_2, median (IQR)		97 (94.75−98.63)
PH		7.43 ± 0.04
PaO_2 (mmHg)		98.79 ± 28.66
Heart rate (/min)		88.47 ± 16.78
Respiratory rate (/min)		20 (20−20)
Systolic pressure (mmHg)		129.1 ± 15.06
Diastolic pressure (mmHg)		82.57 ± 7.65
Pulse pressure (mmHg)		46.57 ± 12.63
Laboratory results		
WBC ($\times 10^9$)	3.5−9.5	5.25 ± 1.96
Neutrophil ($\times 10^9$)	1.8−6.3	2.85 (2.16−4.65)
Lymphocyte ($\times 10^9$)	1.1−3.2	1.00 (0.70−1.80)
Platelet ($\times 10^9$)	125−350	176 (145.5−236.5)
Hemoglobin (g/L)	131−172	134.90 ± 14.98
APTT(s)	22−36	33.57 ± 5.13
PT(s)	10−13.5	12.80 (12.03−13.38)
Fibrinogen (g/L)	2.0−4.0	3.89 ± 0.60
D-dimer (mg/L)	<0.55	0.26 (0.20−0.72)
Blood glucose (mmol/L)	3.9−6.1	6.02 (5.24−7.50)
ALT (U/L)	0−40	22 (17−48)
AST (U/L)	13−40	23 (19−41.5)
LDH(U/L)	12−250	252.5 ± 97.29
TB (umol/L)	3.4−17.1	11.6 (9.10−15.25)
Albumin (g/L)	35−51	39.81 ± 3.78
BUN (mmol/L)	2.6−7.5	3.57 ± 1.12
Creatinine (μmol/L)	41−73	66.52 ± 13.78
Creatine kinase (mmol/L)	40−200	69 (54.75−133.30)
Serum sodium (mmol/L)	135−145	136.4 ± 3.38
Serum potassium (mmol/L)	3.5−5.3	3.40 ± 0.41
Procalcitonin (μg/L)	<0.25	<0.25 (0.05−0.25)
CRP (mg/L)	0.0−6.0	21.10 (5.00−78.48)
ESR (mm/h)	0.0−20.0	30.14 ± 13.88

Tmax, maximal body temperature; SpO_2, arterial blood oxygen saturation; IQR, interquartile range; PaO_2, arterial oxygen partial pressure; WBC, white blood cell; TB, Total bilirubin; APTT, activated partial thrombin time; PT, prothrombin time; ALT, alanine aminotransferase; AST, aspartate aminotransferase; LDH, lactate dehydrogenase; TB, total bilirubin; BUN, blood ureanitrogen; CRP, C reactive protein; ESR, erythrocyte sedimentation rate.

2.3. Imaging data acquisition and semi-quantitative analysis

CT data was acquired using two multidetector imaging machines (Somatom Perspective, Siemens, Germany and Optima CT 540, GE, America). The main scanning parameters were as follows: tube voltage = 120 kVp, tube current (regulated by automatic dose modulation), (30–75) mAs, pitch=(1–1.25)mm, matrix = 512 × 512, slice thickness = 5 mm, FOV = 350 mm × 350 mm. Primary images were reconstructed at a slice thickness of 1–1.25 mm with a lung kernel. All imaging was independently reviewed and evaluated by 2 experienced radiologists (11 and 20 years of experience in thoracic CT) and discrepancies were resolved by consensus. All thin-sectional images (slice thickness of (1.25–1.5) mm) were reviewed on both lung (window width, 1500HU; window level, −700HU) and mediastinal (window width, 350HU; window level, 40HU) settings via picture archiving and communication systems (PACS).

The CT features mainly comprised GGO, mixed GGO and consolidation, with all the terms being defined according to the Fleischner Society [10]. The size of the lesion with diameter less than 1 cm, 1–3 cm, more than 3 cm but less than half of the segment, and more than half of the segment was scored as 1 to 4 point, accordingly [11]. The lesion was assessed segment by segment and the total score ranged from 1 to 72 points. The number of affected lung lobes and segments were also counted.

2.4. Imaging quantification

The quantitative analysis of lung volume infected by COVID-19 was performed by uAI Discover-2019nCoV (Shanghai United Imaging Intelligence Healthcare Co., Ltd.). The software provided the infected region segmentation and quantitative analysis functions. A multi-scale convolutional neural networks was designed to segment both lung and lung infected regions from thin-section chest CT images. During the training stage, a set of CT images of the patients with confirmed COVID-19 pneumonia were collected, and the infected regions were manually delineated by experienced thoracic radiologists. Based on these labeled data, a multi-scale neural network model was trained for the segmentation task. In the application step, the learned model was used to automatically extract lung regions (both lung lobes and segments) and infected regions [12]. A quantitative analysis procedure was performed based on the segmentation results, and the value range of −750 HU to −300 HU and −300 HU to 50 HU was defined as GGO and consolidation, respectively [13,14]. The percentage of the total infection (whole infected regions including but not limited to regions manifested as GGO and consolidation), GGO and consolidation to the whole lung were calculated, accordingly (Fig. 1).

2.5. Statistical analysis

The continuous variables with normal distribution were expressed as a mean standard deviation (SD), while those with abnormal distribution were expressed as a median interquartile range (IQR), and the categorical variables were expressed as a percentage. Correlations between the quantitative and semi-quantitative imaging data, the quantitative imaging data and PSI score, clinical and laboratory data were tested using Spearman's correlation. The correlation coefficient of *rs* (ranging: −1–1) above 0 was considered having a tendency of positive correlation and 1 was considered having perfect correlation. The *rs* below 0 was considered having a tendency of

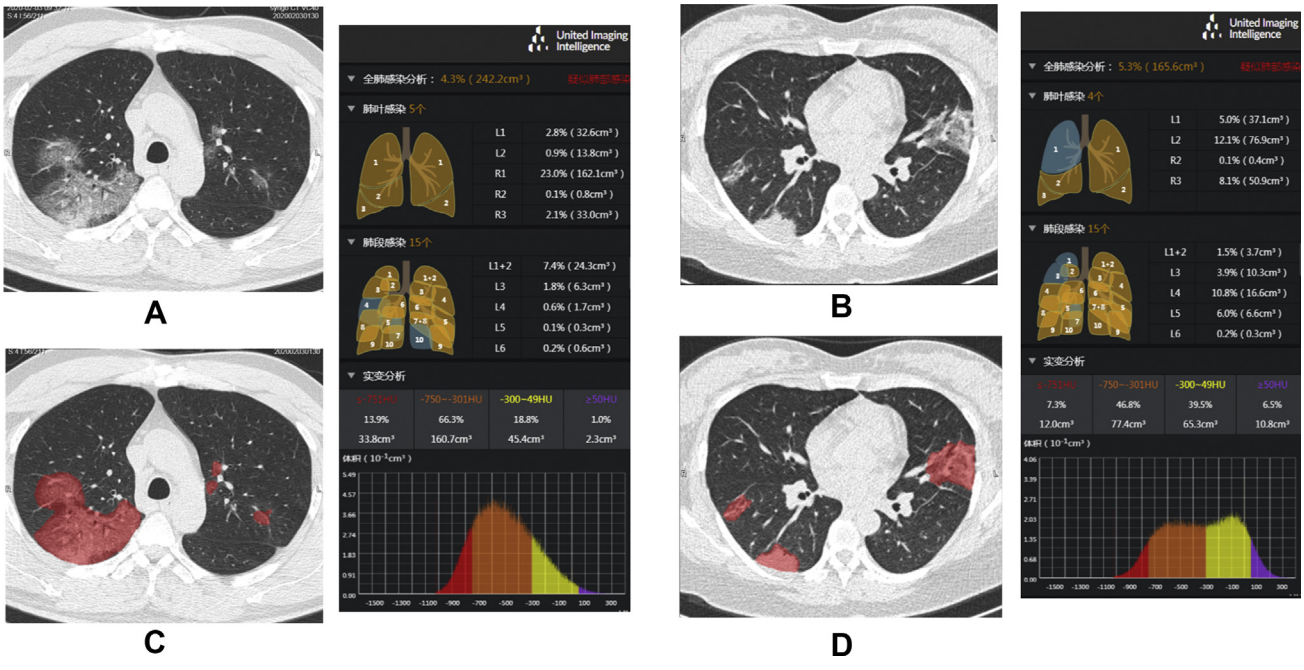

Fig. 1. Auto-segmentation and quantification of the infections by uAI Discover – 2019nCoV: A/C and B/D, unenhanced chest CTs before and after auto-segmentation in a 42-year-old male and a 36-year-old female with COVID-19 pneumonia, respectively. The exported results are presented alongside with detailed information on quantification and histogram.

negative correlation and −1 was considered having perfect negative or inverse correlation [15]. The semi-quantitative and quantitative imaging data between subgroups with different PSI were compared and tested by the unpaired *t*-test. A two-tailed α less than 0.05 was considered as statistically significant. Prism 8 for macOS (version 8.2.1, GraphPad Software, Inc.) was used for all the analyses.

3. Results

3.1. Clinical characteristics

Of the 30 enrolled patients with COVID-19 pneumonia, 16 (53.33%) were male, and the mean age was 48 years old. All patients had a history of direct or indirect contact with people from Wuhan, Hubei province. The interval from onset symptoms to first chest CT scan was 8 days. The common first symptoms were fever, cough and phlegm. Stable vital signs were noticed at admission. The lymphocyte count in 16 (53.33%) cases decreased, while, the C-reactive protein (CRP), erythrocyte sedimentation rate (ESR) and lactate dehydrogenase (LDH) increased in 20 (66.67%), 18 (60%) and 15 (50%) cases respectively. The serum potassium slightly decreased in 18 (60%) cases (Table 1). Sixteen patients (53.33%) were in PSI grade I, 11 patients (36.67%) were in PSI grade II, 2 patients were in PSI grade III, and only 1 patient was in PSI grade Ⅳ (Table 2).

3.2. CT quantification

The semi-quantitative CT score of all the GGO, mixed GGO and consolidation ranged from 1 to 70 in this case series. The total infection detected by the quantitative CT ranged from 0.01% to 39.7%, and the ratio of GGO to consolidation bigger than 1 was seen in 26 patients (86.67%) (Fig. 2 Table 2). The proportion of GGO, consolidation and the total lesion based on the quantitative method was positively correlated with the semi-quantitative CT score ($P < 0.0001$ for all, $rs = 0.88, 0.87, 0.90$), while the ratio of GGO/Consolidation was negatively correlated with the semi-quantitative CT score ($P = 0.0358$, $rs = -0.38$) (Table 3).

3.3. Correlations between quantitative CT and PSI score and laboratory results

The proportion of GGO, consolidation and the total lesion based on the quantitative method was positively correlated with CRP ($P = 0.0278, 0.0168, 0.0078$; $rs = 0.40, 0.43, 0.48$), ESR ($P = 0.0296, 0.0408, 0.0048$; $rs = 0.46, 0.44, 0.58$) respectively, and was negatively correlated with the lymphocyte count ($P = 0.0222, 0.0024, 0.0068$; $rs = -0.42, -0.53, -0.48$). The ratio of GGO/Consolidation was positively correlated with the lymphocyte count ($P = 0.0324$, $rs = 0.39$). The proportion of the total lesion detected by the quantitative method was positively correlated with LDH ($P = 0.0296$, $rs = 0.40$). There were no statistical correlations between the parameters derived from the quantitative method and serum potassium ($P = 0.6044, 0.7528, 0.6076, 0.7636$), and other parameters except the total infection and LDH ($P = 0.0626, 0.0580, 0.4475$). There was a tendency that the percentage of total infection based on quantitative CT positively correlated with the PSI score, although no significantly statistical difference was noticed ($P = 0.0994$; $rs = 0.30$), and no obvious correlations were noticed between the proportion of GGO, consolidation, ratio of GGO/Consolidation and PSI score ($P = 0.1226, 0.1160, 0.6876$), respectively (Table 3).

3.4. Comparisons of semi-quantitative and quantitative CT parameters between patients with different PSI

We classified patients using different grades of PSI into two main subgroups due to the limited case numbers in grade III and Ⅳ: PSI of grade I and PSI of grade II-Ⅳ. The semi-quantitative score, the percentage of GGO, consolidation and total infection in patients with PSI of grade II-Ⅳ was higher than that in patients with PSI of grade I respectively, but there was no statistical difference ($P = 0.2273, 0.1934, 0.0903, 0.0989$). Specifically, there was a trend that both the percentage of consolidation and total infection was higher in patients with PSI of grade II-Ⅳ (Table 4).

Table 2
Baseline CT and PSI score of the 30 patients with COVID-19 Pneumonia.

No.	Quantitative CT				Semi-quantitative CT	PSI Grade (score)
	GGO (%)	Con (%)	GGO/Con	Total (%)		
1	0.52	0.15	3.47	0.7	17	I
2	0.14	0.09	1.56	0.3	3	I
3	2.43	0.9	2.70	3.8	15	II(46)
4	1.86	1.09	1.71	3.2	17	I
5	2.81	2.48	1.13	6.1	29	II(44)
6	0.17	0.08	2.13	0.3	4	I
7	0.11	0.06	1.83	0.2	2	II(69)
8	0.12	0.06	2.00	0.2	1	II(53)
9	8.41e-5	1.12e-5	7.51	0.01	1	I
10	0.62	0.15	4.13	0.9	3	I
11	2.48	2.09	1.19	5.3	25	I
12	0.93	0.14	6.64	1.2	19	I
13	2.85	0.81	3.52	4.3	24	I
14	2.07	1.57	1.32	4.1	16	II(66)
15	1.67	0.95	1.76	2.9	21	II(56)
16	2.95	5.17	0.57	11.2	35	I
17	1.04	0.35	2.97	1.5	7	III(78)
18	24.88	4.08	6.10	39.7	70	II(61)
19	10.20	3.35	3.04	14.6	44	III(77)
20	3.19	5.52	0.58	11.6	38	II(65)
21	14.58	8.5	1.72	26.6	50	IV(92)
22	5.81	4.04	1.44	13.2	44	I
23	7.52	9.14	0.82	21.4	35	II(56)
24	4.25	3.46	1.23	10.0	31	II(58)
25	1.45	0.72	2.01	2.5	7	I
26	0.96	8.44	0.11	21.6	30	II(47)
27	3.13	2.45	1.28	7.5	6	I
28	6.07	5.73	1.06	15.3	43	I
29	0.47	0.16	2.94	0.7	8	I
30	3.07	2.39	1.28	7.2	35	I

Notes: GGO-ground glass opacity, Con-consolidation, PSI-pneumonia severity index.

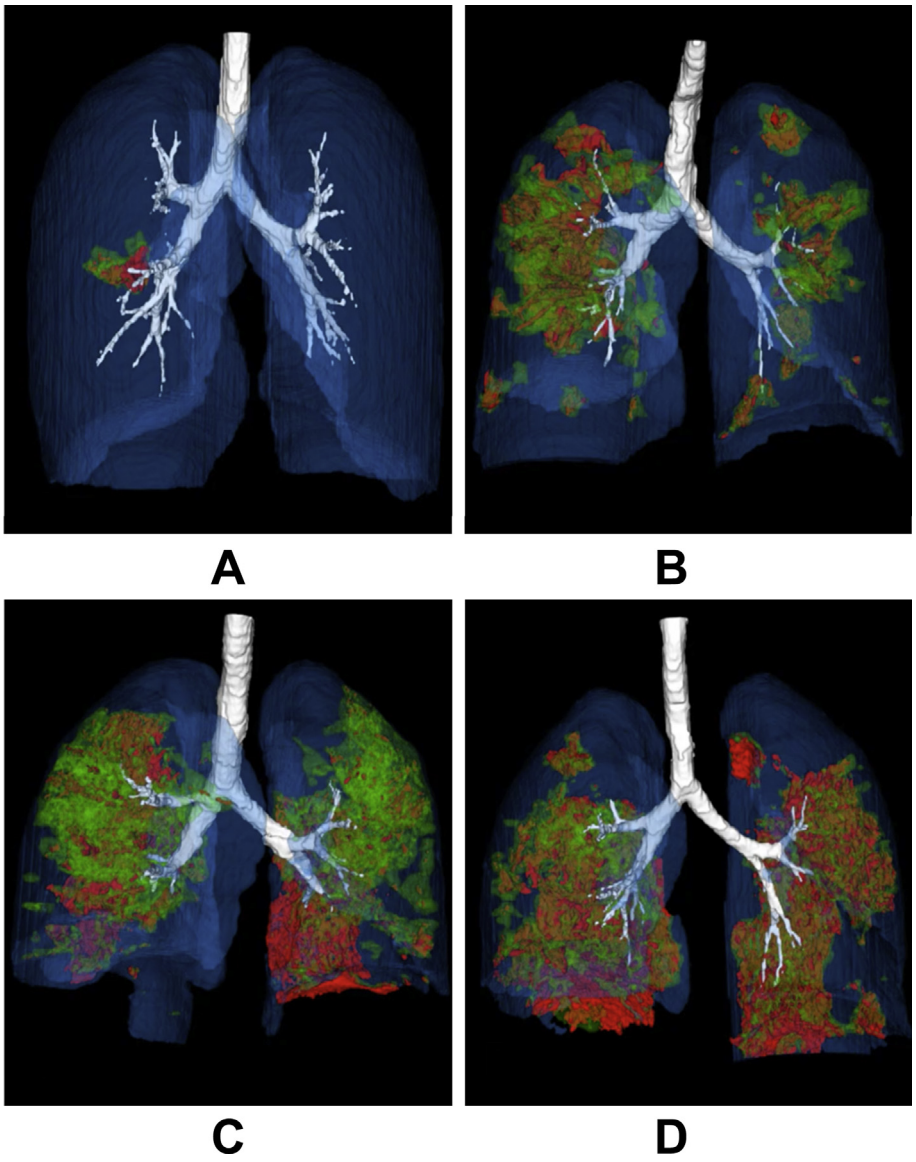

Fig. 2. Three-dimensional volume-rendered reconstructive images showing auto-segmentation of the infected regions based on the quantitative method (anterior to posterior view, the movie is also available in the supplements. Regions in green color stand for ground glass opacity, those in red color stand for consolidation): A, 35 year-old female, with no obvious symptoms, received her first unenhanced chest CT scan 6 days after having contact with people from Wuhan. She was confirmed with COVID-19 pneumonia, and the pneumonia severity index (PSI) was grade I. The infection located in the S6 of the right lower lobe with the visual score of 3 and infection proportion to the whole lung of 0.3%. B, 67 year-old male, fever, cough and chest tightness for 8 days after exposure, received his first unenhanced chest CT scan and confirmed with COVID-19 pneumonia with the PSI of grade III. The infections scattered in all the segments with exception of S10 of the left lower lobe and S7 of the right lower lobe. The visual score was 44 and the infection proportion to the whole lung was 14.6%. C, 46 year-old male, fever, cough, phlegm and muscular ache for 6 days after exposure. He was confirmed with COVID-19 pneumonia with the PSI of grade II. The infections scattered in all the segments with exception of S7+8 of the left lower lobe and S3/S4 of the right upper and middle lobes. The visual score was 35 and the infection proportion to the whole lung was 21.4%. D, 62 year-old male, fever, cough and phlegm for 10 days after exposure. He was confirmed with COVID-19 pneumonia with the PSI of grade IV. The infections scattered in all the segments with exception of S7+8 of the left lower lobe. The visual score was 50 and the infection proportion to the whole lung was 26.6%.

4. Discussion

All participants in our study had direct or indirect contact history with people from Wuhan, there was no doubt that the demographic, epidemiologic and symptomatic characteristics were similar to previous reports from Wuhan [2,1,6]. The lymphocyte decreased in 16 cases, which suggests that COVID-19 shares characteristics with other coronaviruses, such as SARS-CoV and MERS-CoV. The virus can prohibit the cellular immune function by consuming a great deal of immune cells and finally lead to exacerbation of the patients [1,16]. Therefore, the lymphocyte count could be used as a predictor for the severity of the infectious disease. The CRP and ESR elevated in 20 and 18 cases, although they were not specific indexes of infection, the continuously increased level might indicate the co-infections with some other kinds of bacteria and fungi, and the on course of deterioration of the disease. The LDH level increased in half of our cases, which might own to the cardiac and hepatic injury. The LDH reported in critically ill patients was higher than that in the non-

Table 3
Correlations between baseline quantitative CT and semi-quantitative CT, PSI and laboratory results of the 30 patients with COVID-19 pneumonia.

Items	Quantitative CT *p* value *rs* (95%CI)			
	GGO%	Con%	GGO/Con	Total%
Semi-quantitative CT	**<0.0001**	**<0.0001**	**0.0358**	**<0.0001**
	0.88 (0.75, 0.94)	0.87 (0.74, 0.94)	−0.38 (−0.66, −0.02)	0.90 (0.80, 0.95)
PSI	0.1226	0.1160	0.6876	0.0994
	0.28 (−0.09, 0.59)	0.29 (−0.09, 0.60)	−0.08 (-0.43, 0.30)	0.30 (−0.07, 0.61)
Lymphocyte	**0.0222**	**0.0024**	**0.0324**	**0.0068**
	−0.42 (−0.72, −0.14)	−0.53 (−0.75, −0.20)	0.39 (0.03, 0.67)	−0.48 (−0.72, −0.14)
CRP	**0.0278**	**0.0168**	0.4422	**0.0078**
	0.40 (0.04, 0.67)	0.43 (0.08, 0.69)	−0.15 (−0.49, 0.24)	0.48 (0.13, 0.72)
ESR	**0.0296**	**0.0408**	0.2361	**0.0048**
	0.46 (0.04, 0.75)	0.44 (0.01, 0.73)	0.16 (−0.29, 0.56)	0.58 (0.19, 0.81)
LDH	0.0626	0.0580	0.4475	**0.0296**
	0.35 (−0.03, 0.64)	0.36 (−0.02, 0.65)	−0.03 (−0.40, 0.35)	0.40 (0.03, 0.68)
Serum potassium	0.6044	0.7528	0.6076	0.7636
	0.10 (−0.28, 0.45)	0.06 (−0.32, 0.42)	−0.10 (−0.45, 0.28)	0.06 (−0.32, 0.42)

GGO, ground glass opacity; Con, consolidation; PSI, pneumonia severity index; CRP, C reactive protein; ESR, erythrocyte sedimentation rate; LDH, lactate-dehydrogenase, numbers in bold indicating statistical significance.

critically ill patients [2,6], indicating increased LDH might be a predictive index among the hospitalized patients. The serum potassium slightly decreased in 18 cases, which might due to the increased angiotensin II leading to the aldosterone secretion from adrenal cortex, and the increased angiotensin II was found to have a correlation with the severity of the lung infection [17,18]. The total or partial quantitative parameters positively correlated with CRP, ESR and LDH, and negatively correlated with lymphocyte, which implies that the quantification from the baseline chest CT is in accordance with the possible pathophysiological change of the COVID-19 and might be used as a biomarker for assessing the severity of the disease.

PSI is a well-known scoring system for the assessment of the severity of community acquired pneumonia, and has also been verified in application of viral pneumonia [9]. We used PSI as a control to test the potential of the quantitative CT in assessment of the severity and found a tendency of a slight positive correlation between the proportion of total infection and the PSI score although there was no significantly statistical difference. The imbalanced proportion of cases in our study may be the reason for this. Of the 30 patients, 16 were in PSI grade I, and there was no specific score for these cases.

Table 4
Comparisons between patients with COVID-19 pneumonia in different pneumonia severity index (PSI) subgroups.

Characteristics	PSI(I) n = 16	PSI(II-IV) n = 14	*p*
Semi-quantitative score	17 (4.5−32.5)	29.5 (13−39.5)	0.2273
Quantitative parameters			
GGO%	1.66 (0.48−3.04)	2.62 (1.02−8.19)	0.1934
Con%	0.77 (0.14−2.44)	2.92 (0.76−6.25)	0.0903
GGO/Con	1.86 (1.28−3.51)	1.74 (1.05−2.77)	0.3711
Total%	2.85 (0.7−7.43)	8.05 (2.55−21.45)	0.0989

GGO, ground glass opacity; Con, consolidation; %, percentage ofinfected regions (or opacifications) with different CT manifestations to the whole lung volume.

Furthermore, only 2 cases were in PSI grade III and 1 case in PSI grade Ⅳ. Therefore, a more balanced proportional study is warranted in the future. Although the proportion of GGO or consolidation had no correlation with the PCI score, statistically. We should interpret this with caution that these two imaging features stand for different pathological courses, are the manifestations of infection and lung injury, and their dynamic changes might be possible predictors for the prognosis during the follow-up, which needs to be further explored in the following work.

Semi-quantitative score and parameters derived from quantitative CT in patients with higher PSI grades were higher than those in patients with lower PSI grade although there was no statistical difference; similarly, the reason might be limited samples in PSI of grade III and Ⅳ. A more balanced proportion of patients with different grades of PSI are warranted in future investigation to test the possibility of quantitative CT as a potential biomarker in predicting the severity of COVID-19.

The parameters derived from the quantitative method were not only well correlated with the score from the traditional semi-quantitative method but also quantitative of the various imaging features, indicating that this quantitative method might be reliable. Nevertheless, investigations using big data are warranted in order to identify a definite answer.

There were several limitations to this study. Firstly, this was a retrospective study with a small number of cases: this may lead to observer bias and statistical bias; future prospective investigations with a bigger sample are needed. Secondly, we used only baseline clinical and imaging characteristics to complete the correlation tests, which was indirect and insufficient; in addition, most of the cases we included were within mild to moderate grades. Making a prediction for critically ill patients would be of greater significance. There is, therefore, an urgent need to test this quantitative method in future studies with longitudinal observations in a relatively balanced proportion of cases. Thirdly, the segmented infection regions in

this quantitative method may contain small blood vessels, which could affect the results of quantitative analysis. An improved segmentation model would extract these small blood vessels to enable more accurate analysis results.

5. Conclusion

Quantitative chest CT could precisely detect not only the whole volume of the infection but also the proportion of GGO and consolidation. The quantitative method well correlated with the conventional semi-quantitative method, some laboratory indexes relating to viral infection, and PSI. It may have the potential for predicting the severity of the COVID-19 pneumonia immediately after a chest CT on admission.

Funding

This research did not receive any specific grants from funding agencies in the public, commercial, or not-for-profit sectors.

Ethic statement

All procedures performed in studies involving human participants were in accordance with the ethical standards of the institutional and/or national research committee and with the 1964 Helsinki declaration and its later amendments or comparable ethical standards. This article does not contain any studies with animals performed by any of the authors. This study was approved by our Institutional Review Board.

Conflict of interest

None.

References

[1] Chen N, Zhou M, Dong X, Qu J, Gong F, Han Y, et al. Epidemiological and clinical characteristics of 99 cases of 2019 novel coronavirus pneumonia in Wuhan, China: a descriptive study. Lancet 2020;133(9):1025−31.

[2] Huang C, Wang Y, Li X, Ren L, Zhao J, Hu Y, et al. Clinical features of patients infected with 2019 novel coronavirus in Wuhan, China. Lancet 2020;395:497−506.

[3] Li Q, Guan X, Wu P, Wang X, Zhou L, Tong Y, et al. Early transmission dynamics in Wuhan, China, of novel coronavirus-infected pneumonia. N Engl J Med 2020;382:1199−207.

[4] Song F, Shi N, Shan F, Zhang Z, Shen J, Lu H, et al. Emerging coronavirus 2019-nCoV pneumonia. Radiology 2020:200274.

[5] Kanne JP. Chest CT findings in 2019 novel coronavirus (2019-nCoV) infections from Wuhan, China: key points for the radiologist. Radiology 2020:200241.

[6] Wang D, Hu B, Hu C, Zhu F, Liu X, Zhang J, et al. Clinical characteristics of 138 hospitalized patients with 2019 novel coronavirus-infected pneumonia in Wuhan, China. J Am Med Assoc 2020;323(11):1061−9.

[7] Lee KS. Pneumonia associated with 2019 novel coronavirus: can computed tomographic findings help predict the prognosis of the disease? Korean J Radiol 2020;21(3):257−8.

[8] Ko SF, Lee TY, Huang CC, Cheng YF, Ng SH, Kuo YL, et al. Severe acute respiratory syndrome: prognostic implications of chest radiographic findings in 52 patients. Radiology 2004;233(1):173−81.

[9] Kim MA, Park JS, Lee CW, Choi WI. Pneumonia severity index in viral community acquired pneumonia in adults. PloS One 2019;14(3):e0210102.

[10] Hansell DM, Bankier AA, MacMahon H, McLoud TC, Muller NL, Remy J. Fleischner Society: glossary of terms for thoracic imaging. Radiology 2008;246(3):697−722.

[11] Wong KT, Antonio GE, Hui DS, Lee N, Yuen EH, Wu A, et al. Thin-section CT of severe acute respiratory syndrome: evaluation of 73 patients exposed to or with the disease. Radiology 2003;228(2):395−400.

[12] Shan F, Gao Y, Wang J, Shi W, Shi N, Han M, et al. Lung infection quantification of COVID-19 in CT images with deep learning. arXiv:200304655 2020.

[13] Jacobs C, van Rikxoort EM, Twellmann T, Scholten ET, de Jong PA, Kuhnigk JM, et al. Automatic detection of subsolid pulmonary nodules in thoracic computed tomography images. Med Image Anal 2014;18(2):374−84.

[14] Kauczor HU, Heitmann K, Heussel CP, Marwede D, Uthmann T, Thelen M. Automatic detection and quantification of ground-glass opacities on high-resolution CT using multiple neural networks: comparison with a density mask. AJR Am J Roentgenol 2000;175(5):1329−34.

[15] Motulsky HJ. GraphPad statistics guide. 2016. http://www.graphpad.com/guides/prism/7/statistics/index.htm. [Accessed 5 March 2016].

[16] Liu WJ, Zhao M, Liu K, Xu K, Wong G, Tan W, et al. T-cell immunity of SARS-CoV: implications for vaccine development against MERS-CoV. Antivir Res 2017;137:82−92.

[17] Sun ML, Yang JM, Sun YP, Su GH. Inhibitors of RAS might Be a good choice for the therapy of COVID-19 pneumonia. Chinese Journal of Tuberculosis and Respiratory 2020;43:E014. 0.

[18] Zou Z, Yan Y, Shu Y, Gao R, Sun Y, Li X, et al. Angiotensin-converting enzyme 2 protects from lethal avian influenza A H5N1 infections. Nat Commun 2014;5:3594.